A Decentralized Spatial Partitioning Algorithm Based on the Minimum Control Effort Metric

Efstathios Bakolas

***Abstract*— We consider the problem of characterizing a spatial partition of the position space of a team of vehicles with double integrator kinematics. The proximity relations between the vehicles and an arbitrary target point in the partition space is the minimum control effort required for each vehicle to reach the latter point with zero miss distance and exactly zero velocity at a prescribed final time (both the finite and the infinite horizon are considered). We show that the solution to the generalized Voronoi partitioning problem can be associated with a class of affine diagrams whose combinatorial complexity is comparable to the standard Voronoi diagram. For the computation of the latter class of affine diagrams, we utilize a partitioning algorithm, which is decentralized in the sense that each vehicle can compute an approximation of its own cell independently from the other vehicles from the same team. Numerical simulations that illustrate the theoretical developments are also presented.**

I. Introduction

This paper deals with a spatial partitioning problem for a team of vehicles with double integrator kinematics. In particular, each vehicle is associated with a subset of its operating environment, which we refer to as the *Region of Influence* (ROI), in the sense that a target or a task associated with a location within the latter set is automatically assigned to this particular vehicle. In contrast to our previous work on similar partitioning problems, where we have employed centralized computational techniques, in this work, we propose a decentralized partitioning algorithm that allows each vehicle to independently compute its own cell from the partition (or ROI).

The problem considered in this work can be put under the umbrella of generalized Voronoi partitioning problems with respect to *state-dependent* proximity (pseudo-) metrics [1], [2]. In contradistinction with distance functions that stem from geometric considerations solely [3], state-dependent proximity metrics account explicitly for the vehicle dynamics. Partitioning problems with respect to state-dependent metrics for vehicles with single integrator and second order linear dynamics can be found, respectively, in [1], [2], [4]–[6] and [7], [8]. In these references, the proximity metric is taken to be the minimum control effort required for the transition of each vehicle to a neighborhood of a target point with a small terminal speed. In particular, Ref. [7] addresses the partitioning problem by utilizing computational techniques, whereas in [8] it is shown that the same problem can be directly associated with a particular class of power diagrams in higher dimensional partition spaces, for which efficient algorithm exist in the literature. The main drawback of the techniques presented in both [7] and [8] is that they do not allow any vehicle to compute its associated cell independently from the other vehicles from the same team (centralized partitioning algorithms).

In this work, we propose a generalized Voronoi partitioning problem whose proximity metric corresponds to the value function of either a finite horizon minimum control effort problem or an infinite horizon linear optimal control problem with an "observable" quadratic cost. Each vehicle is required to reach an arbitrary target point with zero miss distance and with exactly zero terminal velocity either at a given terminal time (finite horizon) or asymptotically (infinite horizon). In both cases, we show that the characterization of the generalized Voronoi partition reduces to the computation of an affine Voronoi diagram. It is shown that both of the proposed partitioning problems can be addressed by means of a partitioning algorithm, which is *decentralized* in the sense that a vehicle can compute an approximation of its corresponding cell from the partition (or ROI), without computing by itself or receiving any information about the cells that correspond to any other vehicles from the same team. The proposed algorithms build upon some recent results on the parallel computation of generalized Voronoi diagrams in normed spaces by Reem [9], [10].

The rest of the paper is organized as follows. Section II presents the formulation of the optimal control problem for a single vehicle. The partitioning problem is formulated and subsequently solved by means of a decentralized partitioning algorithm in Section III. Section IV presents numerical simulations, and finally, Section V concludes the paper with a summary of remarks.

II. Formulation of the Optimal Steering Problem

We are given a team of n vehicles which are located at n distinct points $\bar{\mathsf{x}}_i \in \mathbb{R}^2$ with prescribed initial velocities $\bar{\mathsf{v}}_i \in \mathbb{R}^2$, where $i \in \mathcal{I}_n := \{1, \ldots, n\}$. We denote by $\overline{\mathcal{X}} := \{\bar{\mathsf{x}}_i \in \mathbb{R}^2 : \ i \in \mathcal{I}_n\}$ and $\overline{\mathcal{V}} := \{\bar{\mathsf{v}}_i \in \mathbb{R}^2 : \ i \in \mathcal{I}_n\}$, respectively, the set comprised of the initial positions and velocities of all the vehicles. The motion of the i-th vehicle from the team, where $i \in \mathcal{I}_n$, is described by the following set of equations

$$\begin{aligned} \dot{\mathsf{x}}_i &= \mathsf{v}_i, & \mathsf{x}_i(0) &= \bar{\mathsf{x}}_i, \\ \dot{\mathsf{v}}_i &= u_i(t), & \mathsf{v}_i(0) &= \bar{\mathsf{v}}_i, \end{aligned} \tag{1}$$

E. Bakolas is an Assistant Professor at the Department of Aerospace Engineering & Engineering Mechanics, The University of Texas at Austin, Austin, Texas 78712-1221, USA, Email: bakolas@austin.utexas.edu

where $\mathsf{x}_i := [x_i,\ y_i]^{\mathrm{T}} \in \mathbb{R}^2$ ($\bar{\mathsf{x}}_i := [\bar{x}_i,\ \bar{y}_i]^{\mathrm{T}} \in \mathbb{R}^2$) and $\mathsf{v}_i := [v_i,\ w_i]^{\mathrm{T}} \in \mathbb{R}^2$ ($\bar{\mathsf{v}}_i := [\bar{v}_i,\ \bar{w}_i]^{\mathrm{T}} \in \mathbb{R}^2$) are, respectively, the position and velocity vectors of the i-th vehicle at time t (at time $t = 0$). In addition, $u_i(\cdot) \in \mathcal{L}^2([0,\infty), \mathbb{R}^2)$ is the control input of the i-th vehicle, where $\mathcal{L}^2([0,\infty), \mathbb{R}^2)$ denotes the space of square integrable functions attaining values in $\mathbb{R}^2$. Furthermore, we denote by $\mathsf{z}_i := [\mathsf{x}_i^{\mathrm{T}},\ \mathsf{v}_i^{\mathrm{T}}]^{\mathrm{T}}$ and $\bar{\mathsf{z}}_i := [\bar{\mathsf{x}}_i^{\mathrm{T}},\ \bar{\mathsf{v}}_i^{\mathrm{T}}]^{\mathrm{T}}$ the state of the i-th vehicle (concatenation of position and velocity vectors) at time t and $t = 0$, respectively. Finally, we denote by $\overline{\mathcal{Z}} := \{\bar{\mathsf{z}}_i \in \mathbb{R}^4 :\ i \in \mathcal{I}_n\}$ the set comprised of the initial positions and velocities of all the vehicles.

Let us now define the *terminal position space* to be the hyperplane $\mathcal{X}_0 := \{[\mathsf{x}_i^{\mathrm{T}},\ \mathsf{v}_i^{\mathrm{T}}]^{\mathrm{T}} \in \mathbb{R}^4 :\ \mathsf{v}_i = 0\}$. Next, we formulate the problem of steering the i-th vehicle from a point in $\overline{\mathcal{Z}}$ to a target point in $\mathcal{X}_0$ as an optimal control problem.

Problem 1 (Finite Horizon): Let $\mathsf{x} \in \mathbb{R}^2$ and let the final time $\tau > 0$ be given. Then, determine a control input $u_i^\circ(\cdot) \in \mathcal{L}^2(\mathbb{R}^2, [0,\infty))$ that minimizes the cost function

$$J(u_i(\cdot)) := \tfrac{1}{2}\int_0^\tau |u_i(t)|^2 \mathrm{d}t \tag{2}$$

subject to the dynamic constraint (1) and the following boundary conditions: $\mathsf{z}_i(0) = \bar{\mathsf{z}}_i$, $\mathsf{z}_i(\tau) = \mathsf{z}(\mathsf{x})$, where $\mathsf{z}(\mathsf{x}) := [\mathsf{x}^{\mathrm{T}},\ 0]^{\mathrm{T}} \in \mathcal{X}_0$.

Problem 1 is a classical minimum control effort problem, whose solution in the special case when x_i is a scalar can be found, for example, in [11]. In our case, it can be shown (the reader is referred to the Appendix for more details) that the optimal control $u_i^\circ(\cdot)$ that solves Problem 1 is a time-varying feedback law, which is given by

$$u_i^\circ(t, \mathsf{x}; \tau, \bar{\mathsf{z}}_i) = \alpha(\mathsf{x}; \tau, \bar{\mathsf{z}}_i) + t\beta(\mathsf{x}; \tau, \bar{\mathsf{z}}_i), \tag{3}$$

where

$$\begin{aligned}\alpha(\mathsf{x}; \tau, \bar{\mathsf{z}}_i) &:= \tfrac{6}{\tau^2}(\mathsf{x} - \bar{\mathsf{x}}_i - \tau\bar{\mathsf{v}}_i) + \tfrac{2}{\tau}\bar{\mathsf{v}}_i,\\ \beta(\mathsf{x}; \tau, \bar{\mathsf{z}}_i) &:= -\tfrac{12}{\tau^3}(\mathsf{x} - \bar{\mathsf{x}}_i - \tau\bar{\mathsf{v}}_i) - \tfrac{6}{\tau^2}\bar{\mathsf{v}}_i.\end{aligned} \tag{4}$$

Note that the gains of the optimal control $u_i^\circ(\cdot)$ depend explicitly on the final time τ. Next, we define the *value function* of the optimal control problem to be the cost $J(u_i^\circ(\cdot))$, where $J(\cdot)$ is defined in Eq. (2). In other words, the value function is the minimum control effort required for the transition of the i-th vehicle from $\bar{\mathsf{z}}_i$ to a point $\mathsf{z}(\mathsf{x}) \in \mathcal{X}_0$, provided that the latter is driven by the optimal control law $u_i^\circ(t, \mathsf{x}; \tau, \bar{\mathsf{z}}_i)$, for $t \in [0, \tau]$. We denote this function by $\mathsf{x} \mapsto J^\circ(\mathsf{x}; \tau, \bar{\mathsf{z}}_i)$, where

$$J^\circ(\mathsf{x}; \tau, \bar{\mathsf{z}}_i) := \tfrac{1}{2}\int_0^\tau |u_i^\circ(t, \mathsf{x}; \tau, \bar{\mathsf{z}}_i)|^2 \mathrm{d}t. \tag{5}$$

As shown in the Appendix, Eqs. (3)-(5) yield

$$J^\circ(\mathsf{x}; \tau, \bar{\mathsf{z}}_i) = \tfrac{6}{\tau^3}|\mathsf{x} - \bar{\mathsf{x}}_i|^2 - \tfrac{6}{\tau^2}\langle \bar{\mathsf{v}}_i, \mathsf{x} - \bar{\mathsf{x}}_i\rangle + \tfrac{2}{\tau}|\bar{\mathsf{v}}_i|^2. \tag{6}$$

Remark 1 Note that as $\tau \to \infty$, then, for every $\mathsf{x} \in \mathbb{R}^2$, both $u_i^\circ(t, \mathsf{x}; \tau, \bar{\mathsf{z}}_i) \to 0$, for all $t \in [0, \tau]$, and $J^\circ(\mathsf{x}; \tau, \bar{\mathsf{z}}_i) \to 0$. Note, however, that the application of an identically zero input will not, in general, steer the i-th to an arbitrary point in $\mathcal{X}_0$. This is a well known problem encountered in minimum control effort problems, which may become ill-posed when the terminal time $\tau \to \infty$.

Proposition 1: The value function of the optimal control Problem 1 can be written as follows

$$J^\circ(\mathsf{x}; \tau, \bar{\mathsf{z}}_i) := \tfrac{6}{\tau^3}|\mathsf{x} - \mathsf{q}(\bar{\mathsf{z}}_i; \tau)|^2 + \delta(\bar{\mathsf{v}}_i; \tau), \tag{7}$$

where $\mathsf{q}(\bar{\mathsf{z}}_i; \tau) := \bar{\mathsf{x}}_i + \frac{\tau}{2}\bar{\mathsf{v}}_i$, and $\delta(\bar{\mathsf{v}}_i; \tau) := \frac{1}{2\tau}|\bar{\mathsf{v}}_i|^2$. In addition, the function $\mathsf{x} \mapsto J^\circ(\mathsf{x}; \tau, \bar{\mathsf{z}}_i)$ attains its minimum value at $\mathsf{x} = \mathsf{q}(\bar{\mathsf{z}}_i; \tau)$. In particular,

$$J^\circ(\mathsf{q}(\bar{\mathsf{z}}_i; \tau); \tau, \bar{\mathsf{z}}_i) = \min_{\mathsf{x} \in \mathbb{R}^2} J^\circ(\mathsf{x}; \tau, \bar{\mathsf{z}}_i) = \delta(\bar{\mathsf{v}}_i; \tau).$$

Proof: From Eq. (6) and by completing the square, we have that

$$\begin{aligned}J^\circ(\mathsf{x}^\circ; \tau, \bar{\mathsf{z}}_i) &= \tfrac{6}{\tau^3}\left(|\mathsf{x} - \bar{\mathsf{x}}_i|^2 - \tau\langle \bar{\mathsf{v}}_i, \mathsf{x} - \bar{\mathsf{x}}_i\rangle + \tfrac{\tau}{4}|\bar{\mathsf{v}}_i|^2\right)\\ &\quad + \tfrac{1}{2\tau}|\bar{\mathsf{v}}_i|^2\\ &= \tfrac{6}{\tau^3}|\mathsf{x} - \bar{\mathsf{x}}_i - \tfrac{\tau}{2}\bar{\mathsf{v}}_i|^2 + \tfrac{1}{2\tau}|\bar{\mathsf{v}}_i|^2.\end{aligned} \tag{8}$$

The result follows readily. ■

A. Infinite Horizon Optimal Control Problem

As we have already mentioned, the minimum control effort problem formulated in Problem 1 becomes ill-posed when $\tau \to \infty$. For this reason, we consider an alternative optimal control problem.

Problem 2 (Infinite Horizon): Let $\mathsf{x} \in \mathbb{R}^2$ be given, and let $0 < \epsilon \ll 1$ be given. Then, determine a control input $u_i^\circ(\cdot) \in \mathcal{L}^2(\mathbb{R}^2, [0,\infty))$ that minimizes the cost function

$$J_\infty(u_i(\cdot); \mathsf{x}) := \tfrac{1}{2}\int_0^\infty \left(\epsilon|\mathsf{z}_i(t) - \mathsf{z}(\mathsf{x})|^2 + |u_i(t)|^2\right)\mathrm{d}t, \tag{9}$$

where $\mathsf{z}(\mathsf{x}) := [\mathsf{x}^{\mathrm{T}},\ 0]^{\mathrm{T}} \in \mathcal{X}_0$, subject to the dynamic constraint (1) and the boundary condition $\mathsf{z}_i(0) = \bar{\mathsf{z}}_i$.

Note that Problem 2 is an infinite horizon linear optimal control problem with an "observable" quadratic cost. It follows (see for example [12]) that the optimal control law $u_i^\circ(\cdot)$ is a (time-invariant) feedback control law, which is given by

$$u_i^\circ(\mathsf{x}; \bar{\mathsf{z}}_i) = -\mathbf{P}(\bar{\mathsf{z}}_i - \mathsf{z}(\mathsf{x})),$$

and the value function $J_\infty^\circ(\mathsf{x}; \bar{\mathsf{z}}_i)$ satisfies the following equation

$$J_\infty(\mathsf{x}; \bar{\mathsf{z}}_i) = \tfrac{1}{2}\langle \mathbf{P}(\bar{\mathsf{z}}_i - \mathsf{z}(\mathsf{x})), \bar{\mathsf{z}}_i - \mathsf{z}(\mathsf{x})\rangle, \tag{10}$$

where $\mathsf{z}(\mathsf{x}) := [\mathsf{x}^{\mathrm{T}},\ 0]^{\mathrm{T}} \in \mathcal{X}_0$ and $\mathbf{P} = \mathbf{P}^{\mathrm{T}} \succ \mathbf{0}$ is a solution to the following Algebraic Riccati Equation (ARE)

$$\mathbf{0} = \mathbf{P}\mathbf{A} + \mathbf{A}^{\mathrm{T}}\mathbf{P} + \mathbf{Q} - \mathbf{P}\mathbf{B}\mathbf{B}^{\mathrm{T}}\mathbf{P} \tag{11}$$

$$\mathbf{A} = \begin{pmatrix}\mathbf{0}_2 & \mathbf{I}_2\\ \mathbf{0}_2 & \mathbf{0}_2\end{pmatrix},\ \mathbf{B} = \begin{pmatrix}\mathbf{0}_2\\ \mathbf{I}_2\end{pmatrix},\ \mathbf{Q} = \epsilon\mathbf{I}_4. \tag{12}$$

Note that actually $\mathbf{P}$ is the unique positive definite solution to the ARE given that the pairs $(\mathbf{A}, \mathbf{B})$ and $(\mathbf{A}, \sqrt{\epsilon}\mathbf{I}_4)$ are, respectively, controllable and observable [12, Problems, 3.2-2, 3.2-4, p. 50].

Proposition 2: Let $\mathbf{P} = \mathbf{P}^{\mathrm{T}} \succ \mathbf{0}$, where

$$\mathbf{P} = \begin{pmatrix} \mathbf{P}_1 & \mathbf{P}_2 \\ \mathbf{P}_2^{\mathrm{T}} & \mathbf{P}_3 \end{pmatrix},$$

where $\mathbf{P}_\ell \in \mathbb{R}^{2\times 2}$, $\ell \in \{1,2,3\}$, be the unique positive-definite solution to the ARE (11). Then,

$$J^\circ_\infty(\mathsf{x};\bar{\mathsf{z}}_i) = \tfrac{1}{2}\langle \mathsf{x} - \mathsf{p}(\bar{\mathsf{z}}_i), \mathbf{P}_1(\mathsf{x} - \mathsf{p}(\bar{\mathsf{z}}_i))\rangle + \mu(\bar{\mathsf{v}}_i), \quad (13)$$

where

$$\begin{aligned} \mathsf{p}(\bar{\mathsf{z}}_i) &:= \bar{\mathsf{x}}_i + \mathbf{P}_1^{-1}\mathbf{P}_2\bar{\mathsf{v}}_i, \\ \mu(\bar{\mathsf{v}}_i) &:= \tfrac{1}{2}\langle \bar{\mathsf{v}}_i, (\mathbf{P}_3 - \mathbf{P}_2^{\mathrm{T}}\mathbf{P}_1^{-1}\mathbf{P}_2)\bar{\mathsf{v}}_i\rangle. \end{aligned} \quad (14)$$

In addition, $J^\circ_\infty(\mathsf{x};\bar{\mathsf{z}}_i)$ attains its minimum value at $\mathsf{x} = \mathsf{p}(\bar{\mathsf{z}}_i)$. In particular,

$$J^\circ_\infty(\mathsf{p}(\bar{\mathsf{z}}_i);\bar{\mathsf{z}}_i) = \min_{\mathsf{x}\in\mathbb{R}^2} J^\circ_\infty(\mathsf{x};\bar{\mathsf{z}}_i) = \mu(\bar{\mathsf{v}}_i).$$

Proof: Because $\mathbf{P} = \mathbf{P}^{\mathrm{T}} \succ 0$, it follows that $\mathbf{P}_1 = \mathbf{P}_1^{\mathrm{T}} \succ 0$. Equation (10) can be written as follows

$$\begin{aligned} J^\circ_\infty(\mathsf{x};\bar{\mathsf{z}}_i) &= \tfrac{1}{2}\big(\langle \bar{\mathsf{z}}_i, \mathbf{P}\bar{\mathsf{z}}_i\rangle + \langle \mathsf{z}(\mathsf{x}), \mathbf{P}\mathsf{z}(\mathsf{x})\rangle\big) - \langle \bar{\mathsf{z}}_i, \mathbf{P}\mathsf{z}(\mathsf{x})\rangle \\ &= \tfrac{1}{2}\big(\langle \bar{\mathsf{z}}_i, \mathbf{P}\bar{\mathsf{z}}_i\rangle + \langle \mathsf{x}, \mathbf{P}_1\mathsf{x}\rangle\big) \\ &\quad - \langle \bar{\mathsf{x}}_i + \mathbf{P}_1^{-1}\mathbf{P}_2\bar{\mathsf{v}}_i, \mathbf{P}_1\mathsf{x}\rangle \\ &= \tfrac{1}{2}\big(\langle \bar{\mathsf{z}}_i, \mathbf{P}\bar{\mathsf{z}}_i\rangle + \langle \mathsf{x}, \mathbf{P}_1\mathsf{x}\rangle\big) \\ &\quad - \langle \mathsf{p}(\bar{\mathsf{z}}_i), \mathbf{P}_1\mathsf{x}\rangle \\ &= \tfrac{1}{2}\langle \bar{\mathsf{z}}_i, \mathbf{P}\bar{\mathsf{z}}_i\rangle \\ &\quad + \tfrac{1}{2}\big(\langle \mathsf{x}, \mathbf{P}_1\mathsf{x}\rangle - 2\langle \mathsf{p}(\bar{\mathsf{z}}_i), \mathbf{P}_1\mathsf{x}\rangle\big) \\ &= \tfrac{1}{2}\big(\langle \bar{\mathsf{z}}_i, \mathbf{P}\bar{\mathsf{z}}_i\rangle - \langle \mathsf{p}(\bar{\mathsf{z}}_i), \mathbf{P}_1\mathsf{p}(\bar{\mathsf{z}}_i)\rangle\big) \\ &\quad + \tfrac{1}{2}\big(\langle \mathsf{x}, \mathbf{P}_1\mathsf{x}\rangle - 2\langle \mathsf{p}(\bar{\mathsf{z}}_i), \mathbf{P}_1\mathsf{x}\rangle \\ &\quad + \langle \mathsf{p}(\bar{\mathsf{z}}_i), \mathbf{P}_1\mathsf{p}(\bar{\mathsf{z}}_i)\rangle\big) \\ &= \tfrac{1}{2}\big(\langle \bar{\mathsf{z}}_i, \mathbf{P}\bar{\mathsf{z}}_i\rangle - \langle \mathsf{p}(\bar{\mathsf{z}}_i), \mathbf{P}_1\mathsf{p}(\bar{\mathsf{z}}_i)\rangle\big) \\ &\quad + \tfrac{1}{2}\langle \mathsf{x} - \mathsf{p}(\bar{\mathsf{z}}_i), \mathbf{P}_1(\mathsf{x} - \mathsf{p}(\bar{\mathsf{z}}_i))\rangle \\ &= \psi(\bar{\mathsf{z}}_i) + \tfrac{1}{2}\langle \mathsf{x} - \mathsf{p}(\bar{\mathsf{z}}_i), \mathbf{P}_1(\mathsf{x} - \mathsf{p}(\bar{\mathsf{z}}_i))\rangle, \end{aligned}$$

where $\psi(\bar{\mathsf{z}}_i) := \frac{1}{2}\big(\langle \bar{\mathsf{z}}_i, \mathbf{P}\bar{\mathsf{z}}_i\rangle - \langle \mathsf{p}(\bar{\mathsf{z}}_i), \mathbf{P}_1\mathsf{p}(\bar{\mathsf{z}}_i)\rangle\big)$. It is easy to show that $\psi(\bar{\mathsf{z}}_i) = \mu(\bar{\mathsf{v}}_i)$ and the result follows readily. ■

III. The Partitioning Problem

Next, we formulate the generalized Voronoi partitioning problem with respect to the value function of the minimum control effort problem, when the final time τ is finite.

Problem 3: Let $\overline{\mathcal{Z}} := \{\bar{\mathsf{z}}_i \in \mathbb{R}^4 : \ i \in \mathcal{I}_n\}$ be given. Then, determine a partition or diagram $\mathfrak{V} = \{\mathfrak{V}_i : \ i \in \mathcal{I}_n\}$ of $\mathcal{X}_0$ such that

1) $\mathcal{X}_0 = \bigcup_{i\in\mathcal{I}_n} \mathfrak{V}_i$,
2) $\operatorname{int}\mathfrak{V}_i \cap \operatorname{int}\mathfrak{V}_j = \varnothing$, for all $i, j \in \mathcal{I}_n$, $i \neq j$,
3) A point $\mathsf{z}(\mathsf{x}) = [\mathsf{x}^{\mathrm{T}}, \ 0]^{\mathrm{T}} \in \mathcal{X}_0$ belongs to $\mathfrak{V}_i$ if, and only if, $J^\circ(\mathsf{x};\tau,\bar{\mathsf{z}}_i) \leq J^\circ(\mathsf{x};\tau,\bar{\mathsf{z}}_j)$, for all $j \in \mathcal{I}_n$, where $J^\circ(\mathsf{x};\tau,\bar{\mathsf{z}}_\ell)$, $\ell \in \{i,j\}$, is given by Eq. (6).

We also consider the partitioning problem, when the time-horizon is infinite.

Problem 4: Address Problem 3 when the proximity metric is the value function of the infinite horizon optimal control problem $J^\circ_\infty(\mathsf{x};\bar{\mathsf{z}}_i)$, which is given by Eq. (13), in lieu of $J^\circ(\mathsf{x};\tau,\bar{\mathsf{z}}_i)$, for $i \in \mathcal{I}_n$.

A. The Finite Horizon Case

Let $\bar{\mathsf{z}}_i$, $\bar{\mathsf{z}}_j \in \overline{\mathcal{Z}}$. Then, their corresponding bisector in $\mathfrak{V}$, that is, the loci of the points $\mathsf{z}(\mathsf{x}) \in \mathcal{X}_0$, where $J^\circ(\mathsf{x};\tau,\bar{\mathsf{z}}_i) = J^\circ(\mathsf{x};\tau,\bar{\mathsf{z}}_j)$, is determined by the following equation

$$\langle \mathsf{x}, \chi(\bar{\mathsf{z}}_i,\bar{\mathsf{z}}_j;\tau)\rangle = m(\bar{\mathsf{z}}_i,\bar{\mathsf{z}}_j;\tau), \quad (15)$$

where

$$\begin{aligned} \chi(\bar{\mathsf{z}}_i,\bar{\mathsf{z}}_j;\tau) &:= \mathsf{q}(\bar{\mathsf{z}}_j;\tau) - \mathsf{q}(\bar{\mathsf{z}}_i;\tau), \\ m(\bar{\mathsf{z}}_i,\bar{\mathsf{z}}_j;\tau) &:= \tfrac{1}{2}(|\mathsf{q}(\bar{\mathsf{z}}_j;\tau)|^2 - |\mathsf{q}(\bar{\mathsf{z}}_i;\tau)|^2) \\ &\quad + \tfrac{\tau^3}{12}(\delta(\bar{\mathsf{v}}_j;\tau) - \delta(\bar{\mathsf{v}}_i;\tau)). \end{aligned}$$

Note that Eq. (15) describes a straight line in $\mathcal{X}_0$.

Proposition 3: Let $\tau > 0$ be given and let $\mathfrak{V} := \{\mathfrak{V}_i, \ i \in \mathcal{I}_n\}$ denote the generalized Voronoi diagram that solves Problem 3 for a given set of generators $\overline{\mathcal{Z}} := \{\bar{\mathsf{z}}_i, \ i \in \mathcal{I}_n\}$. In addition, let $\mathfrak{Q} := \{\mathfrak{Q}_i, \ i \in \mathcal{I}_n\}$ be the generalized Voronoi diagram of $\mathbb{R}^2$ that is generated by the point-set $\overline{\mathcal{Q}} := \{\bar{\mathsf{q}}_i = \mathsf{q}(\bar{\mathsf{z}}_i;\tau), \ i \in \mathcal{I}_n\}$, where $\mathsf{q}(\bar{\mathsf{z}}_i;\tau) := \bar{\mathsf{x}}_i + \tau/2\bar{\mathsf{v}}_i$, with respect to the (generalized) proximity metric $J^\circ : \mathsf{x} \mapsto J^\circ(\mathsf{x};\tau,\bar{\mathsf{q}}_i,\bar{\mathsf{v}}_i)$, where

$$J^\circ(\mathsf{x};\tau,\bar{\mathsf{q}}_i,\bar{\mathsf{v}}_i) := \tfrac{6}{\tau^3}|\mathsf{x} - \bar{\mathsf{q}}_i|^2 + \tfrac{1}{2\tau}|\bar{\mathsf{v}}_i|^2. \quad (16)$$

For a given $\mathsf{x} \in \mathbb{R}^2$, the point $\mathsf{z}(\mathsf{x}) = [\mathsf{x}^{\mathrm{T}}, \ 0]^{\mathrm{T}} \in \mathcal{X}_0$ belongs to the cell $\mathfrak{V}_i \in \mathfrak{V}$ if, and only if, the point x belongs to the cell $\mathfrak{Q}_i \in \mathfrak{Q}$. In addition, $\mathfrak{Q} := \{\mathfrak{Q}_i, \ i \in \mathcal{I}_n\}$ is an affine diagram with combinatorial complexity $\Theta(n)$[1].

Proof: Equations (6) and (16) imply that $J^\circ(\mathsf{x};\tau,\bar{\mathsf{z}}_i) = J^\circ(\mathsf{x};\tau,\bar{\mathsf{q}}_i,\bar{\mathsf{v}}_i)$, provided that $\bar{\mathsf{q}}_i = \mathsf{q}(\bar{\mathsf{z}}_i;\tau)$. Therefore, a point $\mathsf{z}(\mathsf{x}) = [\mathsf{x}^{\mathrm{T}}, \ 0]^{\mathrm{T}} \in \mathcal{X}_0$ belongs to the cell $\mathfrak{V}_i \in \mathfrak{V}$, if, and only if, $J^\circ(\mathsf{x};\tau,\bar{\mathsf{z}}_i) \leq J^\circ(\mathsf{x};\tau,\bar{\mathsf{z}}_j)$, for all $i \neq j$, or equivalently, $J^\circ(\mathsf{x};\tau,\bar{\mathsf{q}}_i,\bar{\mathsf{v}}_i) \leq J^\circ(\mathsf{x};\tau,\bar{\mathsf{q}}_j,\bar{\mathsf{v}}_i)$, where $\bar{\mathsf{q}}_\ell = \mathsf{q}(\bar{\mathsf{z}}_\ell;\tau)$, for $\ell \in \{i,j\}$. Consequently, $\mathsf{z}(\mathsf{x}) \in \mathfrak{V}_i \in \mathfrak{V}$ if, and only if, $\mathsf{x} \in \mathfrak{Q}_i$, where $\mathfrak{Q}_i \in \mathfrak{Q}$.

Finally, the bisector $\mathcal{B}_{ij}$ that corresponds to the pair of generators $(\bar{\mathsf{q}}_i,\bar{\mathsf{q}}_j) \in \overline{\mathcal{Q}} \times \overline{\mathcal{Q}}$, where $i \neq j$, satisfies Eq. (15), which is the equation of a straight line in $\mathbb{R}^2$. Consequently, $\mathfrak{Q}$ is an affine Voronoi diagram in $\mathbb{R}^2$. The result on the combinatorial complexity of $\mathfrak{Q}$ follows immediately from Theorem 18.2.3 in [13, p. 439]. ■

Remark 2 We wish to highlight at this point that the affine diagram $\mathfrak{Q}$ can be computed in $\Theta(n\log n + n)$ time [13]. The previous bound on the time complexity holds provided that one computes the partition by utilizing specialized algorithms for this particular class of partitions, as explained in [13]. Unfortunately, these algorithms are centralized, and consequently, they are not suitable for applications of multi-vehicle systems.

B. The Infinite Horizon Case

In this case, the bisector that corresponds to two generators $\bar{\mathsf{z}}_i$, $\bar{\mathsf{z}}_j \in \overline{\mathcal{Z}}$, that is, the loci of the points $\mathsf{z}(\mathsf{x}) \in \mathcal{X}(0)$

[1]We denote by $\Theta(f(n))$ the set of functions $F : \mathbb{N} \mapsto [0,\infty)$ for which there exist c_1, $c_2 > 0$ and $n_0 \in \mathbb{N}$ such that $c_1 f(n) \leq F(n) \leq c_2 f(n)$, for all $n \geq n_0$.

where $J^\circ_\infty(\mathsf{x};\bar{\mathsf{z}}_i) = J^\circ_\infty(\mathsf{x};\bar{\mathsf{z}}_j)$, is determined by the following equation

$$\langle \mathbf{P}_1(\mathsf{x}-\mathsf{p}(\bar{\mathsf{z}}_i)), \mathsf{x}-\mathsf{p}(\bar{\mathsf{z}}_i)\rangle = \langle \mathbf{P}_1(\mathsf{x}-\mathsf{p}(\bar{\mathsf{z}}_j)), \mathsf{x}-\mathsf{p}(\bar{\mathsf{z}}_j)\rangle + 2\left(\mu(\bar{\mathsf{v}}_j)-\mu(\bar{\mathsf{v}}_i)\right),$$

from which it follows that $\langle \mathsf{x}, \chi_\infty(\bar{\mathsf{z}}_i,\bar{\mathsf{z}}_j)\rangle = m(\bar{\mathsf{z}}_i,\bar{\mathsf{z}}_j)$, where

$$\begin{aligned}\chi_\infty(\bar{\mathsf{z}}_i,\bar{\mathsf{z}}_j) &:= 2\mathbf{P}_1(\mathsf{p}(\bar{\mathsf{z}}_j)-\mathsf{p}(\bar{\mathsf{z}}_i)),\\ m(\bar{\mathsf{z}}_i,\bar{\mathsf{z}}_j) &:= \langle \mathbf{P}_1\mathsf{p}(\bar{\mathsf{z}}_j), \mathsf{p}(\bar{\mathsf{z}}_j)\rangle \\ &\quad - \langle \mathbf{P}_1\mathsf{p}(\bar{\mathsf{z}}_j), \mathsf{p}(\bar{\mathsf{z}}_j)\rangle + 2(\mu(\bar{\mathsf{v}}_j)-\mu(\bar{\mathsf{v}}_i)).\end{aligned}$$

Proposition 4: Let $\tau > 0$ be given, and let $\mathfrak{V} := \{\mathfrak{V}_i,\ i \in \mathcal{I}_n\}$ denote the generalized Voronoi diagram that solves Problem 4 for a given set of generators $\overline{\mathcal{Z}}$. In addition, let $\mathfrak{P} := \{\mathfrak{P}_i,\ i \in \mathcal{I}_n\}$ be the generalized Voronoi diagram in $\mathbb{R}^2$ that is generated by the point-set $\overline{\mathcal{P}} := \{\bar{\mathsf{p}}_i = \mathsf{p}(\bar{\mathsf{z}}_i;\tau),\ i \in \mathcal{I}_n\}$ with respect to the (generalized) proximity metric $J^\circ_\infty : \mathsf{x} \mapsto J^\circ_\infty(\mathsf{x},\bar{\mathsf{p}}_i,\bar{\mathsf{v}}_i)$, where

$$J^\circ_\infty(\mathsf{x};\bar{\mathsf{p}}_i,\bar{\mathsf{v}}_i) = \tfrac{1}{2}\langle \mathbf{P}_1(\mathsf{x}-\bar{\mathsf{p}}_i), \mathsf{x}-\bar{\mathsf{p}}_i\rangle + \mu(\bar{\mathsf{v}}_i),$$

and where $\mathsf{p}(\bar{\mathsf{z}}_i)$ and $\mu(\bar{\mathsf{v}}_i)$ are given by Eq. (14). For a given $\mathsf{x} \in \mathbb{R}^2$, the point $\mathsf{z}(\mathsf{x}) = [\mathsf{x}^{\mathrm{T}},\ 0]^{\mathrm{T}} \in \mathcal{X}_0$ belongs to $\mathfrak{V}_i \in \mathfrak{V}$ if, and only if, $\mathsf{x} \in \mathfrak{P}_i$, where $\mathfrak{P}_i \in \mathfrak{P}$. Finally, $\mathfrak{P} := \{\mathfrak{P}_i,\ i \in \mathcal{I}_n\}$ is an affine diagram with combinatorial complexity $\Theta(n)$.

Proof: The proof is similar to the one of Proposition 3 and is omitted. ■

C. A Decentralized Spatial Partitioning Algorithm

Next, we present a decentralized algorithm, which computes the partition $\mathfrak{V} = \{\mathfrak{V}^i,\ i \in \mathcal{I}_n\}$ that solves Problem 3. Problem 4 can be addressed similarly. In light of Proposition 3, instead of computing the partition $\mathfrak{V}$ of $\mathcal{X}_0$ that is generated by $\overline{\mathcal{Z}} \subset \mathbb{R}^4$, it suffices to compute the partition $\mathfrak{Q}$ of $\mathbb{R}^2$ generated by $\overline{\mathcal{Q}} \subset \mathbb{R}^2$. We will henceforth assume, based on practical considerations, that our partition space is a convex polygon $\mathcal{S} \subset \mathbb{R}^2$.

Before we proceed, we make the following assumption:

Assumption 1: Let $\tau > 0$ and $\overline{\mathcal{X}} = \{\bar{\mathsf{x}}_i,\ i \in \mathcal{I}_n\} \subset \mathrm{int}(\mathcal{S})$ be given. Let also $\bar{\mathsf{q}}_i := \bar{\mathsf{x}}_i + \frac{\tau}{2}\bar{\mathsf{v}}_i$, for $i \in \mathcal{I}_n$. Then, the following condition holds

$$\tfrac{6}{\tau^3}|\bar{\mathsf{q}}_i - \mathsf{q}(\bar{\mathsf{z}}_j;\tau)|^2 + \delta(\bar{\mathsf{v}}_j;\tau) \geq \delta(\bar{\mathsf{v}}_i;\tau), \qquad (17)$$

for all $i \in \mathcal{I}_n$ and $j \in \mathcal{I}_n\backslash\{i\}$.

Remark 3 It is easy to show that when Assumption 1 holds, then the point $\bar{\mathsf{q}}_i \in \overline{\mathcal{Q}}$ will belong to the interior of its corresponding cell $\mathfrak{Q}_i$ from the partition $\mathfrak{Q}$. Note that condition (17) is trivially satisfied when, for example, all the vehicles have the same initial speed, that is, $|\bar{\mathsf{v}}_i| = |\bar{\mathsf{v}}_j|$ for all $i, j \in \mathcal{I}_n$.

Next, we present a partitioning algorithm that takes advantage of the following special property the affine diagram $\mathfrak{Q}$ that solves Problem 3: For each point $\mathsf{x} \in \mathfrak{Q}_i$, the line segment from $\bar{\mathsf{q}}_i$ to x, which is denoted by $[\bar{\mathsf{q}}_i, \mathsf{x}]$, will belong to the cell $\mathfrak{Q}_i$. Conversely, let $\Gamma(\bar{\mathsf{q}}_i, \mathsf{e})$ denote the ray emanating from $\bar{\mathsf{q}}_i$ that is parallel to a vector $\mathsf{e} \in \mathbb{S}^1$, where $\mathbb{S}^1$ denotes the unit circle. Then, if there exists a point $\mathsf{y} \in \Gamma(\bar{\mathsf{q}}_i, \mathsf{e}) \cap \mathrm{int}(\mathfrak{Q}_j)$, for which $J^\circ(\mathsf{y};\tau,\bar{\mathsf{q}}_j,\bar{\mathsf{v}}_j) < J^\circ(\mathsf{y};\tau,\bar{\mathsf{q}}_i,\bar{\mathsf{v}}_i)$, where $j \in \mathcal{I}_n\backslash\{i\}$, then $\Gamma(\mathsf{y},\mathsf{e}) \cap \mathfrak{Q}_i = \varnothing$. Based on the previous observation, we propose an algorithm that, for a given $\mathsf{e} \in \mathbb{S}^1$, seeks for the furthest point in $\Gamma(\bar{\mathsf{q}}_i, \mathsf{e})$ for which $J^\circ(\mathsf{x};\tau,\bar{\mathsf{q}}_i,\bar{\mathsf{v}}_i) \leq J^\circ(\mathsf{x};\tau,\bar{\mathsf{q}}_j,\bar{\mathsf{v}}_j)$, for all $j \in \mathcal{I}_n\backslash\{i\}$. We will denote the latter point, which corresponds to the intersection of the ray $\Gamma(\bar{\mathsf{q}}_i, \mathsf{e})$ with the boundary of the cell $\mathfrak{Q}_i$, by $\mathsf{x}_{\mathrm{bd}}(\mathsf{e},\bar{\mathsf{q}}_i)$. Note that the set $\bigcup_{\mathsf{e}\in\mathbb{S}^1} \mathsf{x}_{\mathrm{bd}}(\mathsf{e},\bar{\mathsf{q}}_i)$ corresponds to the boundary $\mathrm{bd}(\mathfrak{Q}_i)$ of the cell $\mathfrak{Q}_i$.

For the implementation of this algorithm, we first discretize the unit circle $\mathbb{S}^1$ into a mesh of L nodes, call it $\mathcal{E}$. Then, we characterize the point $\mathsf{x}_{\mathrm{bd}}(\mathsf{e},\bar{\mathsf{q}}_i) \in \mathrm{bd}(\mathfrak{Q}_i)$, for each unit vector $\mathsf{e} \in \mathcal{E}$. To this aim, we employ a bisection algorithm similar to the one presented in [9], [10] for the computation of generalized Voronoi partitions in normed spaces. The main steps of the algorithm are described next:

Step 1: Initially, we set $\mathsf{x}_{\mathrm{bd}}(\mathsf{e},\bar{\mathsf{q}}_i) := \mathsf{x}^{[0]}$, where $\mathsf{x}^{[0]} := \Gamma(\bar{\mathsf{q}}_i;\mathsf{e}) \cap \mathrm{bd}(\mathcal{S})$. In addition, we set $\rho^{[0]}(\mathsf{e}) := |\mathsf{q}(\bar{\mathsf{z}}_i) - \mathsf{x}^{[0]}|$ and $\mathcal{J}^{[0]}(\mathsf{e}) := J^\circ(\mathsf{x}^{[0]};\tau,\bar{\mathsf{q}}_i,\bar{\mathsf{v}}_i)$.

Step 2: If $\mathcal{J}^{[0]}(\mathsf{e}) \leq J^\circ(\mathsf{x}^{[0]};\tau,\bar{\mathsf{q}}_j,\bar{\mathsf{v}}_j)$, for all $j \in \mathcal{I}_n\backslash\{i\}$, then we set $\mathsf{x}_{\mathrm{bd}}(\mathsf{e},\bar{\mathsf{q}}_i) := \mathsf{x}^{[0]}$ and we go to step 5). Otherwise, we set $\mathsf{x}^{[1]} := \bar{\mathsf{q}}_i + \rho^{[1]}(\mathsf{e})\mathsf{e}$, where $\rho^{[1]}(\mathsf{e}) := \frac{1}{2}\rho(\mathsf{e})$, and $\mathcal{J}^{[1]}(\mathsf{e}) := J^\circ(\mathsf{x}^{[1]};\tau,\bar{\mathsf{q}}_j,\bar{\mathsf{v}}_j)$.

Step 3: If $\mathcal{J}^{[1]}(\mathsf{e}) \leq J^\circ(\mathsf{x}^{[1]};\tau,\bar{\mathsf{q}}_j,\bar{\mathsf{v}}_j)$, for all $j \in \mathcal{I}_n\backslash\{i\}$, then we set $\rho^{[2]}(\mathsf{e}) := \rho^{[1]}(\mathsf{e}) + \frac{1}{2}(\rho^{[0]}(\mathsf{e}) - \rho^{[1]}(\mathsf{e}))$. Otherwise, we set $\rho^{[2]}(\mathsf{e}) := \rho^{[1]}(\mathsf{e}) - \frac{1}{2}(\rho^{[0]}(\mathsf{e}) - \rho^{[1]}(\mathsf{e}))$. Then, we set $\mathsf{x}^{[2]} := \bar{\mathsf{q}}_i + \rho^{[2]}(\mathsf{e})\mathsf{e}$ and $\mathcal{J}^{[2]}(\mathsf{e}) := J^\circ(\mathsf{x}^{[2]};\tau,\bar{\mathsf{q}}_i,\bar{\mathsf{v}}_i)$.

Step 4: We repeat the steps 1) - 3) until $|\rho^{[k]}(\mathsf{e}) - \rho^{[k-1]}(\mathsf{e})| < \varepsilon$ or $|\mathcal{J}^{[k]}(\mathsf{e}) - \mathcal{J}^{[k-1]}(\mathsf{e})| < \epsilon$, for some given threshold $\varepsilon > 0$ and a positive integer k.

Step 5: We repeat the Steps 1-4, for all the L unit vectors in $\mathsf{e} \in \mathcal{E}$.

The output of the previous procedure will be a point-set $\mathrm{bd}_{\mathcal{E}}(\mathfrak{Q}_i) := \{\mathsf{x} \in \mathcal{S} :\ \mathsf{x} = \mathsf{x}_{\mathrm{bd}}(\mathsf{e},\bar{\mathsf{q}}_i),\ \text{for } \mathsf{e} \in \mathcal{E}\}$, which approximates the boundary $\mathrm{bd}(\mathfrak{Q}_i)$ of the cell $\mathfrak{Q}_i$.

Remark 4 The previously described decentralized, yet approximate (in the sense that the computed partition is an approximation of the actual one), partitioning algorithm has time complexity $\mathcal{O}(n^2)$, where n is the number of vehicles, as is claimed in [9], [10].

Remark 5 Note that the algorithm for the computation of the solution to Problem 4 can be designed similarly by just replacing $\bar{\mathsf{q}}_\ell$ and $\mathcal{J}^\circ(\cdot;\tau,\bar{\mathsf{q}}_\ell,\bar{\mathsf{v}}_\ell)$ in the previous discussion with, respectively, $\bar{\mathsf{p}}_\ell$ and $\mathcal{J}^\circ_\infty(\cdot;\bar{\mathsf{p}}_\ell,\bar{\mathsf{v}}_\ell)$, where $\ell \in \{i, j\}$.

IV. Numerical Simulations

In this section, we present numerical simulations that illustrate the previously presented theoretical developments. In particular, we consider a set $\overline{\mathcal{Z}}$ that consists of ten

generators. Figure 1 illustrates the solutions to Problem 3 for final time $\tau = 2$ (Fig. 1(a)), which corresponds to an affine diagram generated by the point set $\overline{\mathcal{Q}}$, and Problem 4 (Fig. 1(b)), which corresponds to an affine diagram generated by the point set $\overline{\mathcal{P}}$. The red crosses and the black arrows in both Fig. 1(a) and Fig. 1(b) denote, respectively, the initial positions and velocities of all the vehicles. Furthermore, the magenta crosses correspond to the point-sets $\overline{\mathfrak{Q}}$ (Fig. 1(a)) and $\overline{\mathcal{P}}$ (Fig. 1(b)), respectively. Both of the two partitions which are illustrated in Figure 1 have been computed by employing a naive centralized approximation algorithm whose main steps are summarized below: First, we define a uniform, fine grid $\mathcal{G}$ on the partition space (here, we consider a 400×400 grid). Subsequently, we assign to each node of the grid the index of the vehicle that can reach this node with zero terminal speed (exactly or asymptotically, respectively) with smaller transition cost than any other vehicle. Note that this naive partitioning scheme has time complexity $\mathcal{O}(n|\mathcal{G}|)$, where $|\mathcal{G}|$ denotes the cardinality of the grid $\mathcal{G}$, that is, the number of its nodes [14]. Typically, the size of the grid depends on the number of vehicles; the higher the number of vehicles, the finer the grid should be. For example, $|\mathcal{G}|$ should be at least $\mathcal{O}(n^q)$, with $q > 2$. The blue circles centered at points from the set $\overline{\mathcal{X}}$, which are illustrated in both Fig. 1(a) and Fig.1(b), correspond to the level sets of the value function of the finite horizon optimal control problem $\mathcal{J}^\circ(\cdot; \tau, \bar{\mathsf{z}}_i)$ restricted to the cell $\mathfrak{Q}_i \in \mathfrak{Q}$ and the value function of the infinite horizon optimal control problem $\mathcal{J}^\circ_\infty(\cdot; \bar{\mathsf{z}}_i)$ restricted to the cell $\mathfrak{P}_i \in \mathfrak{P}$, respectively, for all $i \in \mathcal{I}_n$. Finally, the green dashed lines correspond to the standard Voronoi diagram generated by the point-set $\overline{\mathcal{X}}$. We observe that both of the affine diagrams differ significantly from their corresponding standard Voronoi diagrams.

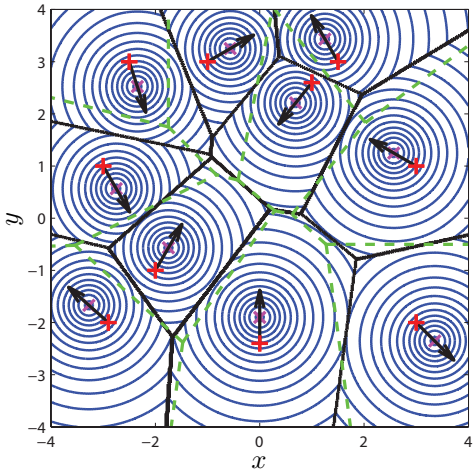

(a) The finite horizon case.

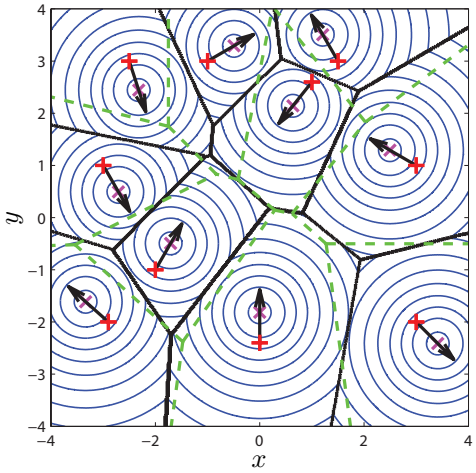

(b) The infinite horizon case.

Fig. 1. Generalized Voronoi diagrams generated by a set of ten points with respect to the minimum control effort metric considering both a finite horizon and infinite horizon. The partitions are computed via a naive centralized approximation algorithm that employs a fine grid (400×400) over the partition space.

Next, we present the results of numerical simulations on the computation of the generalized Voronoi partitions by utilizing the decentralized partitioning algorithm, which was presented in Section III-C. In particular, Fig. 2 illustrates a cell of the partition $\mathfrak{Q}$ (finite horizon problem) which was computed independently by its associated vehicle by means of the decentralized partitioning algorithm. For the computation of this cell, we have discretized the interval $[0, 2\pi)$ into a uniform mesh, $\mathcal{T}$, which induces, in turn, a discretization of the unit circle $\mathbb{S}^1$ into a mesh, $\mathcal{E}$; specifically, each unit vector $\mathsf{e}(\theta) = [\cos\theta, \ \sin\theta]^{\mathrm{T}} \in \mathcal{E}$ corresponds to a $\theta \in \mathcal{T}$, and vice versa. For our simulations, we have considered a coarse grid that consists of 60 nodes (Fig. 2(a)) and a less coarse one (Fig. 2(b)), which consists of 120 nodes. The approximation of the cell obtained with the use of the less coarse grid is actually very close to the one obtained via the naive centralized partitioning algorithm, which is illustrated in Fig. 1(a).

V. Conclusion

In this paper, we have addressed a spatial partitioning problem that is relevant to applications of multi-vehicle systems. The proximity metric of the proposed spatial partition is a state-dependent generalized metric, namely the minimum control effort required to steer a vehicle from a team of vehicles with double integrator kinematics, to a target point with zero miss distance and at zero terminal velocity either at a given final time (finite horizon) or asymptotically (infinite horizon). We have shown that the solution to both problems can be associated with a class of affine diagrams, which can be computed by means of a decentralized partitioning algorithm. In particular, with the utilization of the proposed algorithm, each vehicle can compute its own cell independently from the other vehicles from the same team, that is, without having to compute and / or receive information about the cells of any other vehicle from the same team. Future work includes the design of decentralized partitioning algorithms for problems involving multi-vehicle systems with nonlinear dynamics.

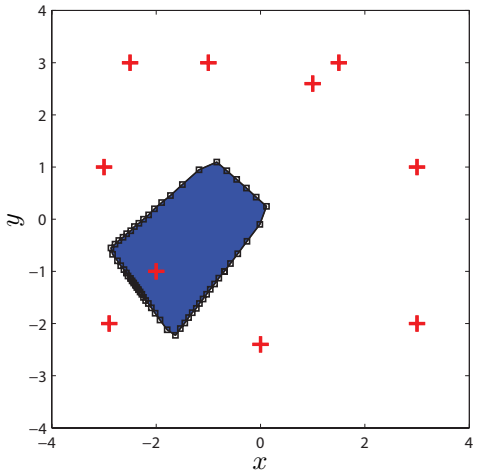

(a) Coarse approximation of a cell of $\mathfrak{Q}$.

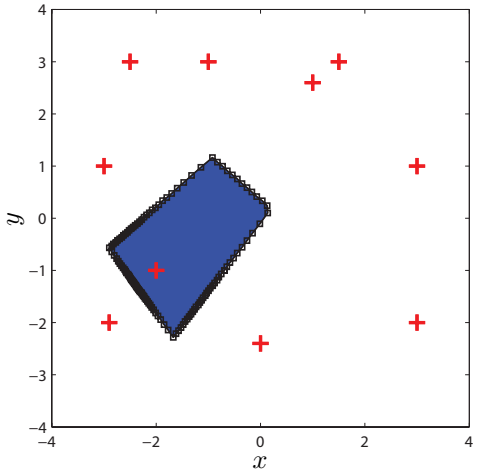

(b) Fine approximation of a cell of $\mathfrak{Q}$.

Fig. 2. A particular cell from $\mathfrak{Q}$ computed via the decentralized partitioning algorithm using a coarse and a fine grid of 60 and 120 nodes, respectively, for the unit circle $\mathbb{S}^1$.

APPENDIX

In this appendix, we briefly discuss the solution of Problem 1 (finite-horizon minimum control effort problem). To this aim, we consider the variational Hamiltonian for Problem 1

$$\mathcal{H}(\lambda_{\mathsf{x}}^i, \lambda_{\mathsf{v}}^i, \mathsf{x}_i, \mathsf{v}_i, u_i) := \tfrac{1}{2}|u_i|^2 + \langle \lambda_{\mathsf{x}}^i, \mathsf{v}_i \rangle + \langle \lambda_{\mathsf{v}}^i, u_i \rangle,$$

where $t \mapsto \lambda_{\mathsf{x}}^i(t)$, $t \mapsto \lambda_{\mathsf{v}}^i(t)$ are absolutely continuous functions, the *costates*, which satisfy the following differential equations

$$\dot{\lambda}_{\mathsf{x}}^i(t) = 0, \quad \dot{\lambda}_{\mathsf{v}}^i(t) = -\lambda_{\mathsf{x}}^i(t).$$

The *stationarity* condition of the optimal control problem,

$$\frac{\partial \mathcal{H}}{\partial u_i}(\lambda_{\mathsf{x}}^i, \lambda_{\mathsf{v}}^i, \mathsf{x}_i, \mathsf{v}_i, u_i) = 0,$$

furnishes the following (candidate) optimal control law

$$u_i^\circ(t) = \alpha + t\beta, \quad \alpha = -\lambda_{\mathsf{v}}^i(0), \quad \beta = \lambda_{\mathsf{x}}^i(0).$$

By integrating Eq. (1) from $t = 0$ to $t = \tau$, we obtain the following equations

$$\mathsf{x} = \mathsf{x}_i(\tau) = \bar{\mathsf{x}}_i + \tau \bar{\mathsf{v}}_i + \tfrac{\tau^2}{2}\alpha + \tfrac{\tau^3}{3}\beta,$$
$$0 = \mathsf{v}_i(\tau) = \bar{\mathsf{v}}_i + \tau\alpha + \tfrac{\tau^2}{2}\beta,$$

which yield, after some algebraic manipulation, the expressions for α and β given in Eq. (4). In addition, by evaluating the cost functional $J(u_i^\circ(\cdot))$, we obtain the following equation for the value function of Problem 1

$$J^\circ(\mathsf{x}; \tau, \bar{\mathsf{z}}_i) = \tfrac{1}{2}\left(\tau|\alpha|^2 + \tau^2\langle\alpha, \beta\rangle + \tfrac{1}{3}\tau^3|\beta|^2\right),$$

which yields Eq. (6).

REFERENCES

[1] E. Bakolas and P. Tsiotras, "The Zermelo-Voronoi diagram: a dynamic partition problem," *Automatica*, vol. 46, no. 12, pp. 2059–2067, 2010.

[2] E. Bakolas and P. Tsiotras, "Optimal partitioning for spatiotemporal coverage in a drift field," *Automatica*, vol. 49, no. 7, pp. 2064–2073, 2013.

[3] A. Okabe, B. Boots, K. Sugihara, and S. N. Chiu, *Spatial Tessellations: Concepts and Applications of Voronoi Diagrams*. West Sussex, England: John Wiley and Sons Ltd, second ed., 2000.

[4] K. Sugihara, "Voronoi diagrams in a river," *International Journal of Computational Geometry and Applications*, vol. 2, no. 1, pp. 29–48, 1992.

[5] K. Sugihara, "Why are Voronoi diagrams so fruitful in application?," in *ISVD 2011*, p. 14, June 2011.

[6] Y. Ru and S. Martinez, "Coverage control in constant flow environments based on a mixed energy-time metric," *Automatica*, vol. 49, no. 9, pp. 2632–2640, 2013.

[7] E. Bakolas, "Optimal partitioning for task assignment of spatially distributed vehicles based on quadratic performance criteria," in *American Control Conference (ACC), 2013*, pp. 3206–3211, 2013.

[8] E. Bakolas, "Optimal partitioning for multi-vehicle systems using quadratic performance criteria," *Automatica*, vol. 49, no. 11, pp. 3377–3383, 2013.

[9] D. Reem, "An algorithm for computing Voronoi diagrams of general generators in general normed spaces," in *ISVD '09*, pp. 144 –152, June 2009.

[10] D. Reem, "On the possibility of simple parallel computing of Voronoi diagrams and Delaunay graphs," *arXiv:1212.1095*, 2012.

[11] A. E. Bryson and Y. C. Ho, *Applied Optimal Control*. Waltham, MA: Blaisdell Publication, 1969.

[12] B. D. O. Anderson and J. B. Moore, *Optimal Control: Linear Quadratic Methods*. Mineola, NY: Dover, 2007.

[13] J.-D. Boissonnat and M. Yvinec, *Algorithmic Geometry*. Cambridge, United Kingdom: Cambridge University Press, 1998.

[14] T. Nishida, S. Ono, and K. Sugihara, "Direct diffusion method for the construction of generalized Voronoi diagrams," in *ISVD 2007*, pp. 145–151, July 2007.